Evaluation of a 4D Cone-Beam CT Reconstruction Approach Using an Anthropomorphic Phantom

Ziv Yaniv[1], Jan Boese[2], Marily Sarmiento[3], and Kevin Cleary[1]

[1] Imaging Science and Information Systems Center, Department of Radiology, Georgetown University Medical Center, Washington, DC, USA
[2] Siemens AG Healthcare, Forchheim, Germany
[3] Siemens AG Healthcare, Malvern, PA, USA

Abstract. We have previously developed image-guided navigation systems for thoracic abdominal interventions utilizing a three dimensional (3D) Cone-Beam CT (CBCT) image acquired at breath-hold. These systems required the physician to perform the intervention in a gated manner, with actions performed at the same respiratory phase in which the CBCT image was acquired. This approach is not always applicable, as many patients find it hard to comply with the breath-hold requirement. In addition the physician's actions are limited to a specific respiratory phase. To mitigate these deficiencies we have developed and implemented a retrospectively gated acquisition protocol using a clinical C-arm based system. The resulting 4D (3D+time) image is then used as input for the navigation system. We evaluate our reconstruction approach using a computer controlled anthropomorphic respiring phantom. The phantom is respired using respiratory rates of 12, 15 and 20 breaths per minute, and three amplitudes corresponding to shallow, normal, and deep breathing patterns. We show that the gated images have a better contrast to noise ratio and sharper edges than the images reconstructed without gating. Thus we are able to acquire an intra-operative data set that potentially provides better navigation accuracy, using 3D images at arbitrary points in the respiratory cycle without requiring the patient to hold their breath during image acquisition.

1 Introduction

The use of image-guided navigation systems has grown in the past decades, as these systems enable minimally invasive interventions, reducing trauma to the patient. To date, these systems have primarily been applied in procedures dealing with rigid or semi-rigid anatomical structures such as those found in orthopedics and neurosurgery. More recently, developers of image-guidance systems have shifted their focus to thoracic-abdominal soft tissue interventions [1–3]. Commercial systems for soft tissue interventions have also started appearing on the market. Examples of such systems are the PercuNav system from Traxtal Inc., a Philips Heathcare Company, (Toronto Canada) and the iGuide CAPPA system from Siemens AG Healthcare (Erlangen, Germany).

N. Navab and P. Jannin (Eds.): IPCAI 2010, LNCS 6135, pp. 147–156, 2010.

These systems provide guidance based on a three dimensional (3D) image, usually, diagnostic quality CT or MR. This requires that patients hold their breath during image acquisition and that the intervention be carried out at the same respiratory phase in which the image was acquired. As a result, the intervention is performed in a gated manner, with actions limited to a specific respiratory phase. Most often the end expiration phase is used as this is the respiratory phase that has the best reproducibility [4].

Improvements in flat panel detector technology have led to the introduction of interventional C-arm based Cone Beam CT (CBCT) systems that provide reconstructions with sufficient soft tissue resolution for various interventional procedures [5]. By replacing the use of diagnostic CT with C-arm based CBCT the complexity of a procedure's workflow is potentially reduced. Instead of acquiring the CT images in a separate location and transferring the patient to the interventional suite, both imaging and intervention are carried out in the same location.

Based on our experience developing image-guidance systems that utilize either CT or CBCT [3], we conclude that the current guidance approach is sub-optimal for thoracic-abdominal interventions. In many cases, patients are not cooperative and cannot hold their breath during image acquisition. This is often due to sedation or their underlying medical condition. When this is not an issue, subsequent breath-holds after image acquisition do not always correspond to the same respiratory phase, reducing the guidance accuracy.

C-arm based CBCT systems can potentially be used to acquire 4D (3D+time) images. The acquisition and use of a 4D CBCT image for navigation guidance removes the requirement for breath-hold during image acquisition, and will potentially improve navigation accuracy. Instead of an image corresponding to a specific respiratory phase, the system uses images that reflect the position of underlying anatomical structures throughout the respiratory cycle. We are currently pursuing this research with the aim of using 4D CBCT to guide radiofrequency ablation of large (>3cm) tumors in the liver.

A straightforward approach to 4D CBCT acquisition is gated reconstruction. The acquired projection images are binned according to their respiratory phase or amplitude after which 3D reconstructions are performed separately for each bin [6]. This approach requires a dense spatio-temporal sampling. That is, each bin must contain enough spatial information such that it does not trade motion artifacts for reconstruction artifacts due to a sparse spatial sampling along the gantry's trajectory. When using clinical C-arm based systems, scan times are most often less than 30s. These systems are designed for fast rotations, as the intended image acquisition protocols assume patients hold their breath. This results in a sparse spatial sampling if projection images are binned according to a respiratory signal, leading to reconstruction artifacts. This is slightly less of an issue for CBCT systems used in radiation therapy. These on-board systems typically have rotation times longer than 1min.

A theoretical improvement over straightforward gating was presented in [7], using a 3D motion compensated reconstruction approach. This approach assumes

the availability of a pre-operative 4D motion model that is consistent with the intra-operative respiratory motion. This approach was later successfully used in the radiation therapy setting, with 1min CBCT gantry rotation and motion models derived from 4D CT [8]. This approach is not applicable for most image-guided interventions as no pre-operative motion model is available.

We next describe our proposed 4D CBCT reconstruction method using a clinical C-arm system and its evaluation, using a computer controlled anthropomorphic respiring phantom.

2 Materials and Methods

In this work we use the Axiom Artis dFA (Siemens AG Healthcare, Erlangen, Germany) clinical C-arm based CBCT system. We have previously shown, in a simulation study, that a C-arm rotation of 80s using this system's calibration parameters would yield a 4D gated reconstruction of sufficient quality [9]. Unfortunately, the system design is such that it cannot be slowed down. It is optimized for fast rotations, with the longest possible rotation time being 25s. This is insufficient for a gated reconstruction approach as the spatial sampling associated with each respiratory phase is very sparse due to the limited number of respiratory cycles sampled in 25s.

Given the acquisition properties of our system we adopted the reconstruction approach proposed in [10] for reconstruction of gated cardiac images. In that approach the C-arm performs multiple back and forth sweeps. In our case, the C-arm performs five 25s sweeps. In each sweep 166 images are acquired uniformly covering an orbit of 200^o. In total, 830 images are acquired in 125s. This specific choice of number of sweeps and number of images per sweep was based on the maximal size of the hardware's image buffer. It should be noted that the back and forth motions are only approximately identical. We ignore these minor differences during reconstruction and use the same C-arm parameters irrespective of the direction of rotation.

After acquiring the projective images, they are retrospectively labeled with a label in $[-1, 1]$ using the amplitude of a respiratory signal obtained from the motion of a fiducial marker placed on the patient's skin. The signal is estimated from the fiducial's location in the projection images and is thus implicitly synchronized with image acquisition [11]. Unlike the standard hard binning approach where each projection image is associated with one respiratory phase we use the soft binning approach as described in [10]. That is, for every bin, defined by the respiratory signal, we use all 166 C-arm poses. For each pose we select the projection image that is closest to the desired respiratory amplitude. This approach strikes a balance between reducing reconstruction and motion artifacts. Finally, each of the 3D images from the 4D CBCT image is obtained using the system's filtered backprojection reconstruction.

To evaluate our gated reconstruction approach we use a computer controlled anthropomorphic respiring phantom. The phantom anatomy is based on the visible human data. The thorax encloses two cavities that serve as artificial lungs

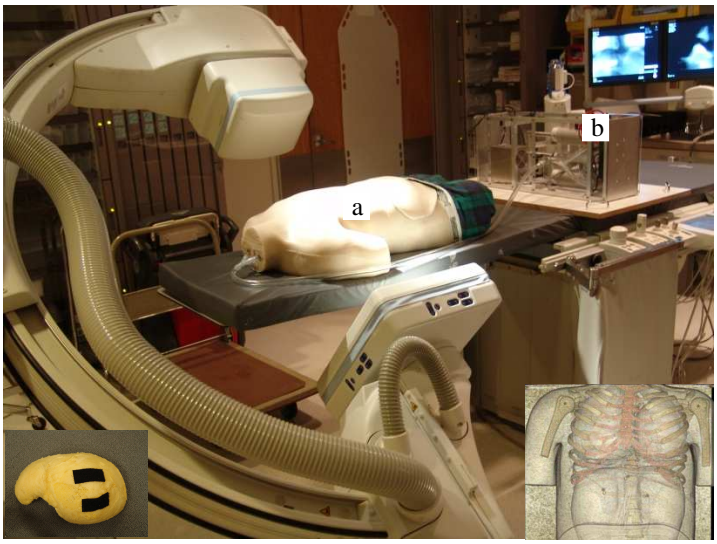

Fig. 1. Experimental setup (a) anthropomorphic respiring phantom and (b) computer controlled pump. Insets show volume rendering from a CT scan of the phantom and the foam liver placed inside the phantom's abdomen.

and artificial organs are placed inside the abdominal cavity [12]. Respiratory motion of the abdominal organs is induced by the motion of the diaphragm as air is pumped into and removed from the lung cavities. Respiration rate and volume are set using a computer controlled pump [13]. Given that our clinical application is navigated liver RFA, we place a foam liver model with a simulated tumor into the phantom's abdomen. This is our object of interest. It should be noted that the phantom only approximates respiratory motion and does not mimic the attenuation coefficients of human tissue.

For evaluation nine data sets were acquired. These correspond to three respiratory rates slow, medium, and fast, 12, 15 and 20 breaths per minute, and respiratory volumes representing shallow, normal and deep breathing. Figure 1 shows our experimental setup and a volume rendering of the phantom. In addition we acquired a CT scan (Siemens Somatom Sensation) and a CBCT scan with the phantom at rest. These serve as a gold standard, the best possible image quality obtained by these imaging systems.

The tumor was manually segmented in the 3D reconstructions. The segmentation is used as input for our evaluation. We use two image quality measures to evaluate reconstructions, Contrast to Noise Ratio (CNR) and the Gradient Magnitude in an Annulus (GM-A) defined by the segmentation boundary. The former assesses general image quality while the later reflects the influence of motion on the reconstruction. If the gating approach removes the blurring due to motion then the CNR is expected to change slightly as it is measured across the whole region of interest, tumor and surrounding tissue. The gradient magnitude

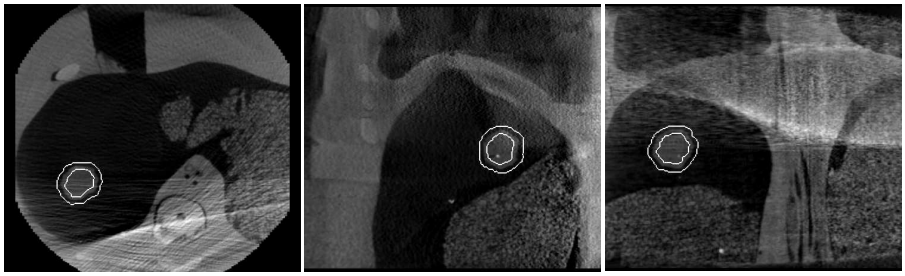

Fig. 2. Axial, Sagittal, and Coronal reformatted images of the anthropomorphic phantom with 3D annulus in which we compute the gradient magnitude

on the other hand is only evaluated at the border of the tumor and is expected to be more sensitive to the removal of motion blurring. On the other hand if the gating scheme introduces noise artifacts into the reconstruction then the CNR is expected to be lower and the gradient magnitude is expected to be higher. As a consequence these two quality values should be considered in conjunction, with the ideal results reflecting both higher CNR and gradient magnitude. Finally we also compare the estimated tumor size with and without gating to the size estimated by the segmentation of the stationary CT data.

The CNR formula we use is defined in [14]:

$$CNR = \frac{|\mu_{fg} - \mu_{bg}|}{\sqrt{(\sigma_{fg}^2 + \sigma_{bg}^2)/2}}$$

In our case the simulated tumor inside the foam liver serves as our foreground. The background is automatically defined by dilating the segmented tumor such that the volume of the surrounding background is approximately equal to the tumor volume.

Our second quality measure, GM-A, is defined by the segmentation boundary. This quality measure allows us to evaluate the effect of our gated reconstruction on motion artifacts, as these result in blurred object boundaries. To reduce the dependency on accurate tumor segmentation we evaluate the gradient magnitude in a 5mm annulus defined by the manual segmentation, as illustrated in Figure 2.

Finally, we compare the effect of our reconstruction approach on the estimated tumor volume, with the ground truth tumor volume obtained from a CT of the stationary phantom.

We compare the set of 3D images obtained from our 4D reconstruction approach to the standard 3D reconstruction. In our case we use the 166 projection images acquired in the first sweep of our multi-sweep acquisition as input to the standard 3D reconstruction approach. The input is thus similar to that acquired using the current clinical acquisition method and a freely breathing patient, without the need to perform a separate scan.

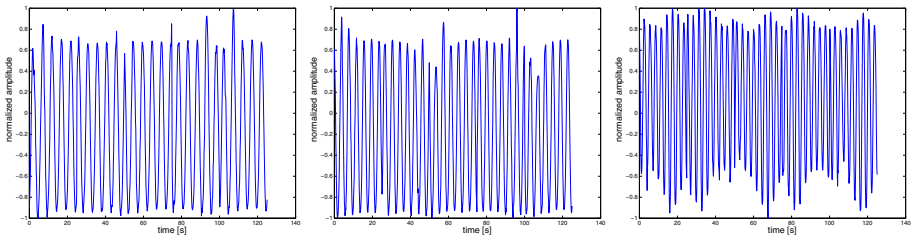

Fig. 3. Sample respiratory signals estimated from the projection images. These correspond, from left to right, to phantom respiration rates of 12, 15, and 20 breaths per minute.

3 Results

When working with our computer controlled respiring phantom we first confirmed that in all cases the respiratory signal obtained from the projection images was indeed consistent with the known respiratory pattern. This is illustrated in Figure 3.

We first visually evaluated our approach to generating a 4D CBCT data set by selecting coronal and sagittal reformatted images from the same spatial location of a 3D image created by our method and that created using the first C-arm sweep. Figure 4 illustrates this qualitative evaluation. In all cases our method was able to improve the visual quality of the data, primarily in the region of the diaphragm.

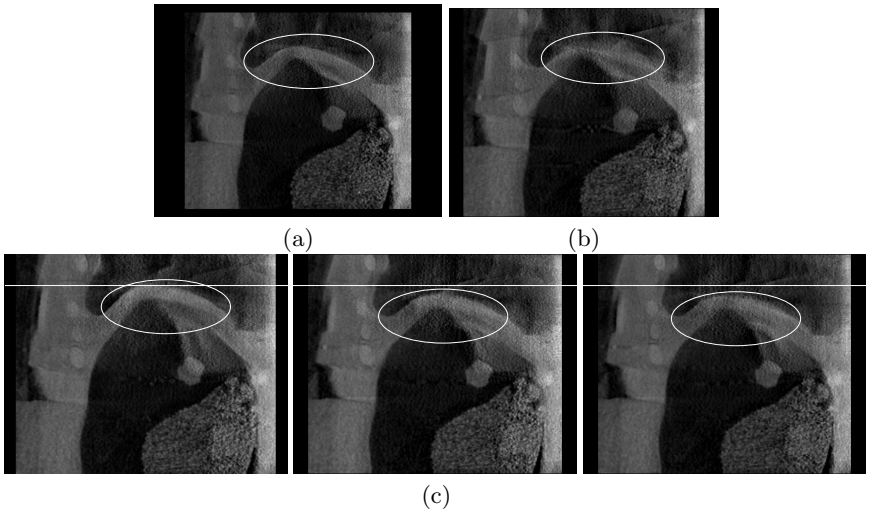

Fig. 4. Reformatted sagittal slices at the same spatial location (a) reconstruction from stationary phantom (b) reconstruction from free breathing data and (c) three respiratory phases reconstructed from gated data. Improved image quality is clearly evident next to the diaphragm (ellipse). The respiratory phases are visible with respect to the line placed at the top of the diaphragm location in the first image.

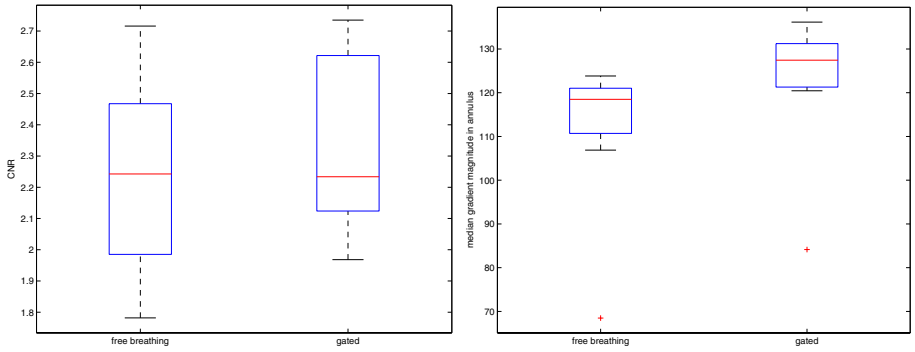

(a) (b)

Fig. 5. Comparison of (a) contrast to noise ratio and (b) median gradient magnitude in annulus, between reconstructions performed using the first sweep of the C-arm in our multi-sweep approach and a gated sweep. Standard values used in plot construction, box spans interquartile range, median marked inside box and maximal whisker length is set to 1.5 times inter quartile range.

We then quantitatively evaluated the 3D image quality obtained by our method and a 3D image obtained using the standard approach, ignoring the phantom's breathing. We start by assessing our ground truth data, a CBCT acquisition of the stationary phantom. The CNR for our ground truth is 2.85 and the GM-A is 117.43.

Figure 5 summarizes the evaluation for both our image quality measures, CNR and GM-A. The results show that the quality of the 3D images that comprise the 4D image is higher than that of the 3D image reconstructed from data that does not compensate for the respiratory motion. We also observed that for shallow breathing our approach does not improve the results irrespective of the respiratory rate but that for normal and deep breathing the results are improved for all respiratory rates, as summarized in Table 1.

Finally, we compared the estimated tumor volumes to the ground truth volume obtained from a CT of the stationary phantom. In our case the ground truth tumor volume is 10243.5mm^3. The median (std) error for the free breathing data was 262.10 (765.16)mm^3 and for the gated data it was 208.60(118.66)mm^3.

Table 1. Quantitative results from all nine data sets as a function of the respiratory rate and volume for corresponding gated(free breathing) data sets (a) CNR values and (b) median GM-A values

	shallow	normal	deep
slow	2.23(2.55)	2.72(2.32)	2.14(2.01)
medium	2.74(2.72)	2.29(2.24)	2.13(1.78)
fast	2.10(2.44)	2.59(2.21)	1.97(1.92)

(a)

	shallow	normal	deep
slow	134.33(119.60)	121.56(112.92)	84.14(68.47)
medium	123.27(123.83)	129.39(118.49)	120.45(106.88)
fast	127.44(123.53)	130.19(120.18)	136.15(111.96)

(b)

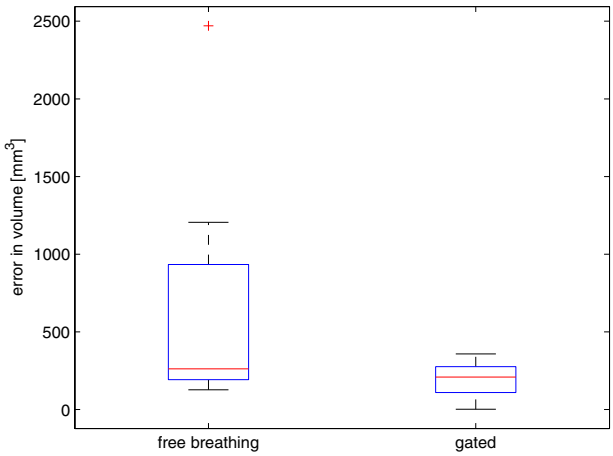

Fig. 6. Errors in tumor volume estimation as compared to a gold standard obtained from a CT of the stationary phantom. Standard values used in plot construction, box spans interquartile range, median marked inside box and maximal whisker length is set to 1.5 times inter quartile range.

Figure 6 summarizes this evaluation. Based on these results we conclude that our gating approach improves the volumetric estimation.

4 Discussion and Conclusion

We have presented a method for retrospective respiratory gating and 4D (3D+time) image reconstruction using an intra-operative C-arm based CBCT system. The proposed method was evaluated using a computer controlled anthropomorphic respiring phantom. We have shown that the proposed approach is able to compensate for the respiratory motion, producing a set of 3D images of improved quality over that available when performing reconstruction that ignores respiratory motion. This study has also shown that 4D CBCT can be readily acquired using currently deployed clinical systems without the need for any hardware modifications.

The use of such a 4D data set will enable data acquisition without requiring the patient to hold their breath during the process. In addition during the intervention breath-holds at arbitrary respiratory phases are accommodated, potentially improving targeting accuracy.

To date, the majority of phantom studies evaluating the effect of respiratory motion have utilized linear stages onto which objects with sharp edges were mounted (e.g. cubes, spheres). In this study we used an anthropomorphic respiring phantom that mimics abdominal respiratory motion. Abdominal motion is affected by the phantom's diaphragm, moving an anatomically correct model of the liver containing a tumor. This results in more realistic motion patterns.

While the end result is closer to human respiratory motion, our study was only conducted using uniform respiratory rates and amplitudes. As this study was an initial evaluation of our proposed reconstruction approach, we did not evaluate the effects of varying respiration rates and volumes during image acquisition. This further evaluation is planned for the near future. It should be noted that our phantom does not exhibit hysteresis and thus cannot fully mimic respiratory motion.

While in most cases our approach improved image quality, for shallow breathing it did reduce it, both for slow and fast respiratory rates. This is most likely due to the minimal motion, approximately 1mm, exhibited by our object of interest. It should be noted that in humans the motion magnitude is much larger, closer to that obtained by our normal, approximately 5mm, and deep breathing, approximately 10mm, motions.

Even with the improved image quality obtained by our method, it is still slightly lower than the image quality obtained when the phantom was stationary. Finally, when compared to diagnostic CT the quality of the images of the stationary phantom was considerably higher in CT with a CNR of 5.08 versus a CNR of 2.85 in the CBCT image. Thus, while the capability of C-arm based CBCT systems to differentiate between different materials has greatly improved it is still not at the level of diagnostic CT.

In thoracic-abdominal interventions, a pre-operative CT is most often available. We are currently investigating the use of this CT in conjunction with the intra-operative 4D CBCT. By registering the CT to each of the 3D images comprising the 4D CBCT image we will be able to provide 4D guidance with the high image quality of diagnostic CT.

Acknowledgement. This work was funded by NIH/NIBIB grant R01EB007195. The authors would like to thank Emmanuel Wilson for his help with the experiments.

References

1. Mundeleer, L., Wikler, D., Leloup, T., Warzée, N.: Development of a computer assisted system aimed at RFA liver surgery. Comput. Med. Imaging Graph. 32(7), 611–621 (2008)
2. Nicolau, S., Pennec, X., Soler, L., Buy, X., Gangi, A., Ayache, N., Marescaux, J.: An augmented reality system for liver thermal ablation: Design and evaluation on clinical cases. Medical Image Analysis 13(3), 494–506 (2009)
3. Yaniv, Z., Cheng, P., Wilson, E., Popa, T., Lindisch, D., Campos-Nanez, E., Abeledo, H., Watson, V., Cleary, K., Banovac, F.: Needle-based interventions with the image-guided surgery toolkit (IGSTK): From phantoms to clinical trials. IEEE Trans. Biomed. Eng. 57(4), 922–933 (2010)
4. Kimura, T., Hirokawa, Y., Murakami, Y., Tsujimura, M., Nakashima, T., Ohno, Y., Kenjo, M., Kaneyasu, Y., Wadasaki, K., Ito, K.: Reproducibility of organ position using voluntary breath hold method with spirometer during extracranial stereotactic radiotherapy. International Journal of Radiation Oncology, Biology, Physics 60(4), 1307–1313 (2004)

5. Wallace, M.J., Kuo, M.D., Glaiberman, C., Binkert, C.A., Orth, R.C., Soulez, G.: Three-dimensional C-arm cone-beam CT: Applications in the interventional suite. Journal of Vascular and Interventional Radiology 19(6), 799–813 (2008)
6. Li, T., Xing, L., Munro, P., McGuinness, C., Chao, M., Yang, Y., Loo, B., Koong, A.: Four-dimensional cone-beam computed tomography using an on-board imager. Med. Phys. 33(10), 3825–3833 (2006)
7. Li, T., Schreibmann, E., Yang, Y., Xing, L.: Motion correction for improved target localization with on-board cone-beam computed tomography. Phys. Med. Biol. 51(2), 253–267 (2006)
8. Rit, S., Wolthaus, J., van Herk, M., Sonke, J.J.: On-the-fly motion-compensated cone-beam CT using an a priori motion model. In: Medical Image Computing and Computer-Assisted Intervention, pp. 729–736 (2008)
9. Hartl, A., Yaniv, Z.: Evaluation of a 4D cone-beam CT reconstruction approach using a simulation framework. In: International Conference of the IEEE Engineering in Medicine and Biology Society (EMBC), pp. 5729–5732 (2009)
10. Lauritsch, G., Boese, J., Wigström, L., Kemeth, H., Fahrig, R.: Towards cardiac C-Arm computed tomography. IEEE Trans. Med. Imag. 25(7), 922–934 (2006)
11. Wiesner, S., Yaniv, Z.: Respiratory signal generation for retrospective gating of cone-beam CT images. In: SPIE Medical Imaging: Visualization, Image-Guided Procedures, and Display (2008)
12. Mazilu, D., et al.: Synthetic torso for training in and evaluation of urologic laparoscopic skills. J. Endourol. 20(5), 340–345 (2006)
13. Lin, R., Wilson, E., Tang, J., Stoianovici, D., Cleary, K.: A computer-controlled pump and realistic anthropomorphic respiratory phantom for validating image-guided systems. In: SPIE Medical Imaging: Visualization and Image-Guided Procedures, vol. 6509 (2007)
14. Perry, N., Broeders, M., de Wolf, C., Törnberg, S., Holland, R., von Karsa, L. (eds.): European guidelines for quality assurance in breast cancer screening and diagnosis (2006)